PLOS ONE

RESEARCH ARTICLE

Methylene-tetrahydrofolate reductase contributes to allergic airway disease

Kenneth R. Eyring[1], Brent S. Pedersen[1], Kenneth N. Maclean[2], Sally P. Stabler[1], Ivana V. Yang[1], David A. Schwartz[1,3]*

1 Department of Medicine, School of Medicine, University of Colorado, Aurora, CO, United States of America, **2** Department of Pediatrics, School of Medicine, University of Colorado, Aurora, CO, United States of America, **3** Department of Immunology, School of Medicine, University of Colorado, Aurora, CO, United States of America

* david.schwartz@ucdenver.edu

Check for updates

OPEN ACCESS

Citation: Eyring KR, Pedersen BS, Maclean KN, Stabler SP, Yang IV, Schwartz DA (2018) Methylene-tetrahydrofolate reductase contributes to allergic airway disease. PLoS ONE 13(1): e0190916. https://doi.org/10.1371/journal.pone.0190916

Editor: Jorg Tost, Institut de genomique, FRANCE

Received: February 2, 2017

Accepted: December 22, 2017

Published: January 12, 2018

Copyright: © 2018 Eyring et al. This is an open access article distributed under the terms of the Creative Commons Attribution License, which permits unrestricted use, distribution, and reproduction in any medium, provided the original author and source are credited.

Data Availability Statement: All DNA methylation and expression data files are available from the GEO database (accession numbers GSE71821, GSE71822, and GSE71823).

Funding: This work was supported by the National Institute of Health, National Institute of Environmental Health Sciences, PO1-ES18181 (http://www.niehs.nih.gov/) to DA and the National Institute of Health, National Heart, Lung, and Blood Institute, RO1-HL101251 (http://www.nhlbi.nih.gov/) to DA and IVY. The funders had no role in

Abstract

Rationale

Environmental exposures strongly influence the development and progression of asthma. We have previously demonstrated that mice exposed to a diet enriched with methyl donors during vulnerable periods of fetal development can enhance the heritable risk of allergic airway disease through epigenetic changes. There is conflicting evidence on the role of folate (one of the primary methyl donors) in modifying allergic airway disease.

Objectives

We hypothesized that blocking folate metabolism through the loss of methylene-tetrahydrofolate reductase (Mthfr) activity would reduce the allergic airway disease phenotype through epigenetic mechanisms.

Methods

Allergic airway disease was induced in C57BL/6 and C57BL/6$^{Mthfr-/-}$ mice through house dust mite (HDM) exposure. Airway inflammation and airway hyperresponsiveness (AHR) were measured between the two groups. Gene expression and methylation profiles were generated for whole lung tissue. Disease and molecular outcomes were evaluated in C57BL/6 and C57BL/6$^{Mthfr-/-}$ mice supplemented with betaine.

Measurements and main results

Loss of Mthfr alters single carbon metabolite levels in the lung and serum including elevated homocysteine and cystathionine and reduced methionine. HDM-treated C57BL/6$^{Mthfr-/-}$ mice demonstrated significantly less airway hyperreactivity (AHR) compared to HDM-treated C57BL/6 mice. Furthermore, HDM-treated C57BL/6$^{Mthfr-/-}$ mice compared to HDM-treated C57BL/6 mice have reduced whole lung lavage (WLL) cellularity, eosinophilia, and Il-4/Il-5 cytokine concentrations. Betaine supplementation reversed parts of the HDM-induced allergic airway disease that are modified by Mthfr loss. 737 genes are differentially expressed and 146 regions are differentially methylated in lung tissue from HDM-treated

study design, data collection and analysis, decision to publish, or preparation of the manuscript.

Competing interests: The authors have declared that no competing interests exist.

C57BL/6$^{Mthfr-/-}$ mice and HDM-treated C57BL/6 mice. Additionally, analysis of methylation/expression relationships identified 503 significant correlations.

Conclusion

Collectively, these findings indicate that the loss of folate as a methyl donor is a modifier of allergic airway disease, and that epigenetic and expression changes correlate with this modification. Further investigation into the mechanisms that drive this observation is warranted.

Introduction

The prevalence of asthma has been increasing over the past several decades [1, 2], and currently, 12.9% of the United States population have been diagnosed with asthma [3]. This increase in prevalence is likely due to environmental exposures as these changes have occurred too rapidly to be explained by genetics alone. Environmental influences play a major role in both the development and progression of asthma [4–7]. These environment-phenotype interactions are beginning to be better understood through increasing research in epigenetic modifications [8–13].

Epigenetic mechanisms are the biological processes that lead to heritable changes in gene expression [14, 15] which are important for cell differentiation, X-chromosome inactivation, genomic imprinting, and other vital cellular responses [14]. Many of these epigenetic processes are dependent on the availability of methyl groups from S-adenosyl methionine (SAM). Single carbon metabolism is the metabolic pathway that maintains SAM levels in the cell (Fig 1A). This includes the re-methylation of homocysteine to methionine with either the co-substrate 5-methyl-tetrahydrofolate or betaine. An imbalance in single carbon metabolism can lead to changes in downstream methylation [16, 17], as well as changes in allergic airway disease (unpublished data).

Methylene tetrahydrofolate reductase (MTHFR) converts 5, 10-methylene-tetrahydrofolate to 5-methyl-tetrahydrofolate which is the folate form used in homocysteine re-methylation. The most common polymorphism in *MTHFR* is the C677T SNP and homozygous TT individuals have a diminished level of global methylation compared to homozygous CC individuals [18]. While a Danish group initially found no association of *MTHFR* C677T with various outcome variables of asthma and atopic disease [19], in a subsequent larger study an increased prevalence of doctor-diagnosed asthma was observed in individuals homozygous for the minor T allele [20]. The TT genotype was also found to be associated with asthma in an Asian population [21]. In addition, children with the minor T allele and higher folate levels had an increased risk of eczema by age 4, but not wheezing or asthma [22].

While our group (unpublished data) and others [23, 24] have demonstrated a causal relationship between *in utero* exposure to methyl donors and both Th_2 immunity and allergic airway disease in mice, the contribution of folate to allergic airway disease has yet to be determined due to the conflicting published data in human cohorts. Thus, we hypothesized that blocking folate metabolism through the loss of Mthfr activity would reduce the severity of allergic airway disease.

Materials and methods

Mice

C57BL/6$^{Mthfr-/-}$ [25] were provided by Rima Rozen (McGill University) and were rederived at Charles River Laboratories. C57BL/6 mice were obtained through Charles River Laboratories.

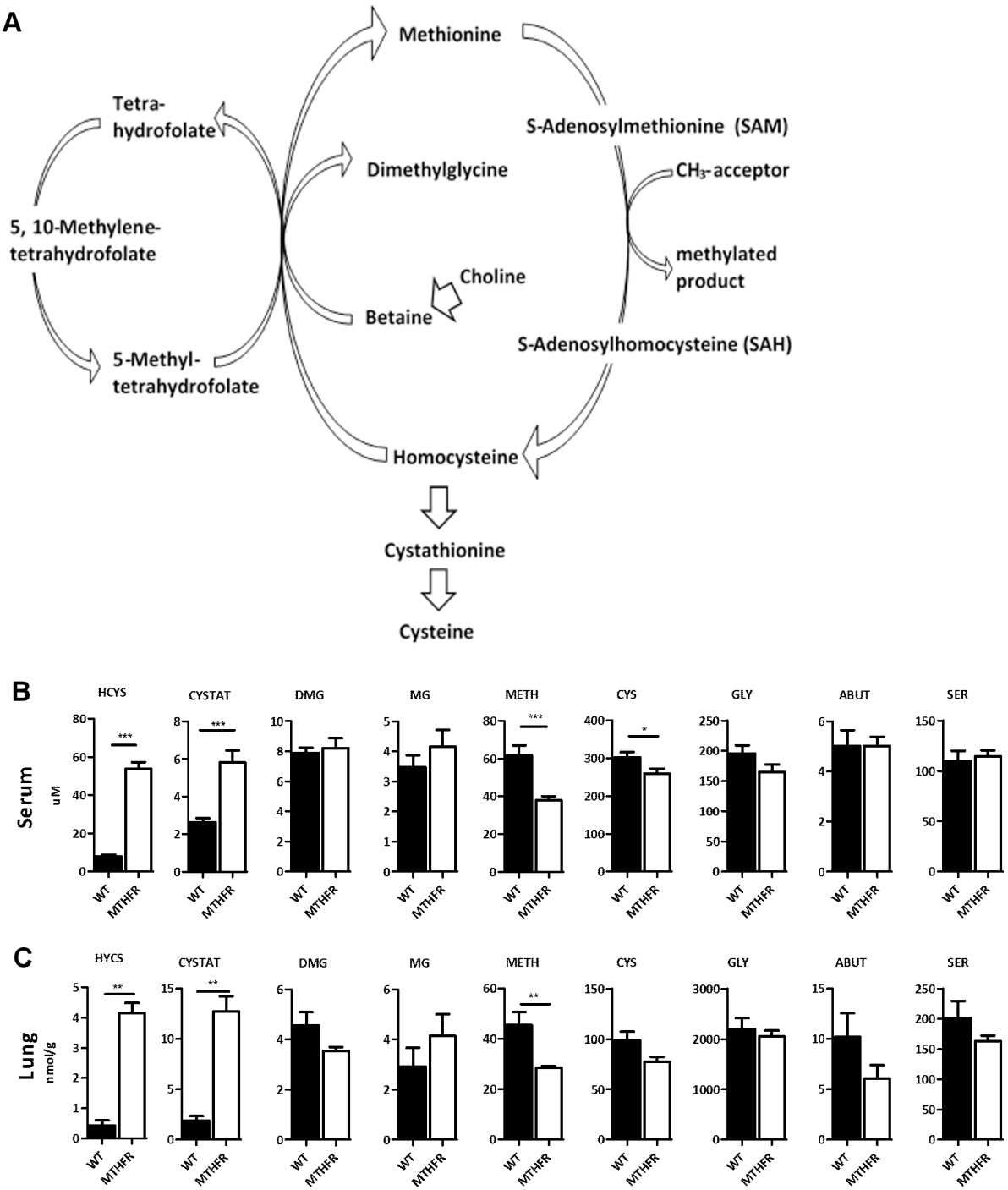

Fig 1. Single carbon metabolite levels differ between C57BL/6$^{Mthfr-/-}$ and C57BL/6 mice. (A) Single Carbon metabolism pathway. C57BL/6$^{Mthfr-/-}$ mice demonstrate altered levels of single carbon metabolites (homocysteine, HCYS; cystathionine, CYSTAT; dimethylglycine, DMG; methylglycine, MG; methionine, METH; cysteine, CYS; glycine, GLY; alpha aminobutyrate, ABUT; serine, SER) in (B) serum and (C) whole lung tissue compared to C57BL/6 mice (C57BL/6 black bars; C57Bl/6$^{Mthfr-/-}$ white bars, * p-value <0.05, *** p-value <0.001).

https://doi.org/10.1371/journal.pone.0190916.g001

Animals were housed under standard conditions and protocols were approved by the Institutional Animal Care and Use Committee of the University of Colorado.

Phenotyping

Mice were sensitized to 10 μg of filtered house dust mite extract (HDM, GREER Labs) or saline through i.p. injection on days 0 and 7 followed by challenge on days 14 and 15 with 5 μg HDM or saline administered intratracheally using a microsprayer (Penn Century). HDM was reconstituted in saline to 1 ug/ml and passed through a 0.45 μm filter then a 0.02 μm filter to facilitate microsprayer use. On day 17, mice were anesthetized by an i.p. injection of pentobarbital sodium (60 mg/kg). Following tracheostomy, pancuronium bromide (0.25 mg/kg) was administered, and mice were ventilated on a small animal ventilator (flexiVent FV-FXM1; SCIREQ). Airway resistance was measured through forced oscillation techniques (flexiVent FV-FXM1; SCIREQ) over increasing doses of methacholine (0, 12.5, 25, and 50 mg/ml).

After methacholine challenge, blood and whole lung lavage (WLL) were collected. The lavage fluid was a preparation of 50 mL of 1x phosphate buffered saline (PBS) with 60 μL of 0.5M EDTA added. Mice were lavaged with an initial 1 mL of lavage fluid followed by two consecutive lavages of 0.5 mL of fresh lavage fluid. WLLF was kept on ice throughout processing.

WLLF was then spun down and the supernatant was collected into a separate tube and stored at -80˚C. The cell pellet was then treated with red blood cell lysing buffer (Sigma), spun down, supernatant removed, and resuspended in 1 mL of fresh 1x PBS. Then, cells were counted and total cells were calculated. Slides were prepared and stained with hematoxylin and eosin. After drying, 200 cells were identified and counted based on staining and morphology.

WLL supernatant was concentrated using Amicon Ultra 3K device. Total volume of the WLLF was concentrated by a factor of 3 on average.

Blood was withdrawn through cardiac puncture. It was collected in lithium heparin tubes (BD Inc.). Tubes were spun down at 1000 x g for 10 minutes. Serum was then removed and snap frozen in liquid nitrogen and stored at -80˚C.

Lung tissue was then perfused with PBS and snap frozen. Cytokines in the lung lavage and IgE in the serum were measured using ELISA MAX Standard Sets and protocols from BioLegend.

Betaine supplementation

Betaine (20g/L) was administered as previously published [26] from day -7 to day 17. Anhydrous Betaine (Sigma-Aldrich) was dissolved in drinking water (20 g/l) and was supplied ad libitum from day -7 to day 17 of the HDM sensitization and challenge protocol. Twice per week, Betaine supplemented water was restocked.

Metabolite analysis

Homocysteine, cystathionine, dimethylglycine, methylglycine, methionine, cysteine, serine, glycine, and alpha aminobutyrate were measured in the serum and whole lung tissue through capillary stable isotope dilution gas chromatography/ mass spectrometry.

Agilent expression array

Sample preparation and array processing. A minimum of 25 ng of high quality total RNA from whole lung tissue, as determined by Bioanalyzer RNA assays, was used for SurePrint G3 8x60K arrays (Agilent). One-Color Microarray-Based Gene Expression Analysis: Low Input Quick Amp Labeling protocol version 6.6 and kits were used for this expression experiment. First, RNA was incubated with Spike-in mix, T7 primer, and a cDNA master mix to generate labeled cRNA then purified using RNeasy columns (Qiagen). Then, cRNA was

quantified on NanoDrop Spectrometer to determine total concentration and Cyanine 3 dye concentration. 600 ng of labeled sample was then fragmented then hybridized to the arrays for 17 hours followed by washing. Scanning was modified to meet the specifications of the NimbleGen MS200 scanner. A custom parameter on the NimbleGen MS200 scanner was developed in order to scan the Agilent arrays. Images were uploaded to Feature Extraction 11.5.11 software to extract data.

Analysis. Extracted features were up-loaded into Partek Genomics Suite (Partek Inc.), then underwent quantile normalization and log-2 transformation. Analysis of variance (ANOVA) was applied to determine differences between all experimental groups. Adjusted p-values were generated using the FDR q-value selection through Partek.

Bisulfite sequencing and data analysis

To measure DNA methylation in whole lung tissue, bisulfite sequencing was performed utilizing Agilent's SureSelect Methyl-Seq Target Enrichment System for Illumina Multiplexed Sequencing. Experimental procedures followed SureSelect Human Methyl-Seq Protocol Version B using SureSelect Methyl-Seq Reagent Kit and Mouse Methyl-Seq Capture Library. 4 μg of starting DNA was used for the assay. A final DNA concentration of 2nM per library was submitted for sequencing on the Illumina HiSeq. Each sample was sequenced twice.

Bisulfite-sequencing reads (S1 Table) were trimmed and aligned to the mouse genome *mm10* using *bwa-meth* [27] which also tabulated percent methylation at each CpG motif. Correlating sets of adjacent CpG sites were clustered together using the Adjacent Site Clustering algorithm [28]. Each cluster was required to have a minimum of three CpG sites to constitute a cluster. Methylation clusters were analyzed using a beta regression weighted on sequence read depth, and multiple testing correction was performed using the Benjamini-Hocheberg method [29].

Analysis of DNA methylation and gene expression relationships

A beta regression between methylation loci and expression probes was performed to determine the relationship between methylation and expression data from HDM-treated C57Bl/6$^{Mthfr-/-}$ mice and HDM-treated C57BL/6 mice. Analysis was performed on 6,927 methylation clusters with an uncorrected p-value$<$0.05 unique to the comparison between HDM-treated C57Bl/6$^{Mthfr-/-}$ mice and HDM-treated C57BL/6 mice and all expression probes within 1 Mb of a methylation cluster (54,611). We fit methylation data to expression data and adjusted for Mthfr status.

Pyrosequencing

Differentially methylated regions (DMRs) identified through bisulfite sequencing were confirmed through pyrosequencing PCR on Qiagen's Pyromark MD. Primers for the PCR reaction were designed using the Pyromark Assay Design software (S7 Table). Extracted DNA samples were bisulfite converted using Zymo EZ DNA Methylation-Gold kits and protocol. Unmethylated and methylated controls were included for each primer set. Methylation measurements were averaged across duplicates then across experimental group.

Quantitative RT-PCR

Differential expression was confirmed through qRT-PCR using TaqMan assays (Life Technologies). RNA was converted to cDNA using Superscript III Reverse Transcriptase (Life Technologies) kit and protocol. cDNA was then mixed with TaqMan Fast Advanced Master Mix

and best coverage TaqMan assays then run in triplicate on the ViiA 7 Real-Time machine. Delta CT values were generated from the reference gene, beta-actin.

Statistics

Data were expressed as mean ±SEM. Individual comparisons between groups were confirmed by a 2-tailed Mann-Whitney U test in all cases except for betaine supplementation experiments, where a 1-tailed test was used because we were testing only 1 outcome, that betaine restores the phenotype. Pyrosequecning and qRT-PCR data were analyzed using a 1-tailed Mann-Whitney U test. Significant differences between groups were identified by analysis of variance. GraphPad Prism version 5.04 (GraphPad Software, La Jolla, CA) was used to perform statistical calculations. Pathway analysis was performed using Ingenuity Pathway Analysis (IPA) software. Data deposited in the GEO database (GS71823, http://www.ncbi.nlm.nih.gov/geo/query/acc.cgi?token=odetoocutfgvjyd&acc=GSE71823).

Results

Loss of Mthfr activity altered metabolite levels in single carbon metabolism

Loss of Mthfr activity altered single carbon metabolite concentrations (Fig 1B and 1C). C57BL/6$^{Mthfr\text{-}/\text{-}}$ mice showed a significant increase in serum homocysteine (HYCS) and cystathionine (CYSTAT) while methionine (METH) and cysteine (CYS) are decreased compared to C57BL/6 mice (Fig 1B). These changes in the serum corresponded with those in whole lung tissue for HYCS, CYSTAT, and METH (Fig 1C). These results are due to the loss of co-substrate 5-methyl-tetrahydrofolate hindering the re-methylation of HYCS to METH. Although betaine is a co-substrate and available in the re-methylation of homocysteine, alone it is insufficient in maintaining normal levels of HYCS and METH in the absence of 5-methyl-tetrahydrofolate. HDM treatment had no effect on metabolite levels.

Suppressed allergic airway disease is observed in C57BL/6$^{Mthfr\text{-}/\text{-}}$

HDM-treated C57BL/6$^{Mthfr\text{-}/\text{-}}$ mice demonstrated a suppressed allergic airway disease phenotype compared to HDM-treated C57BL/6 mice including reduced AHR (Fig 2A) and decreased cellularity and eosinophilia in WLL (Fig 2B–2D). Furthermore, HDM-treated C57BL/6$^{Mthfr\text{-}/\text{-}}$ mice showed a significant reduction in Il-4, Il-5, and Il-13 cytokine concentrations in the WLL compared to HDM-treated C57BL/6 mice (Fig 2E–2G). However, serum total IgE levels did not follow this pattern (Fig 2H). Interestingly, HDM-treated C57BL/6$^{Mthfr\text{-}/\text{-}}$ mice had higher levels of total IgE compared to HDM-treated C57BL/6 mice (Fig 2H). Further studies are necessary to elucidate the mechanism of this finding. No statistical differences between saline-treated C57BL/6$^{Mthfr\text{-}/\text{-}}$ and saline-treated C57BL/6 mice were observed for AHR, cellular recruitment, and cytokine levels suggesting that differences in disease state are not a result of a shift in baseline levels except for total IgE levels in the serum while not significant similar differences were present (Fig 2).

HDM-treated C57BL/6 mice were phenotypically different in all measurements compared to saline-treated C57BL/6 mice including an increase in AHR and cellularity, eosinophilia, and cytokine concentrations in the WLL (Fig 2). HDM-treated C57BL/6$^{Mthfr\text{-}/\text{-}}$ mice only differed from the saline-treated C57BL/6$^{Mthfr\text{-}/\text{-}}$ mice by the number and percentage of eosinophils in the WLL (Fig 2). Additionally, detected Ifn-γ in saline-treated mice suggests a slight Th1 bias which is skewed toward Th2 upon HDM-treatment though less extensively in HDM-treated C57BL/6$^{Mthfr\text{-}/\text{-}}$ mice (S1 Fig). However, the HDM response is not skewed toward Treg or Th17 since Il-10 and Il-17 were not detected.

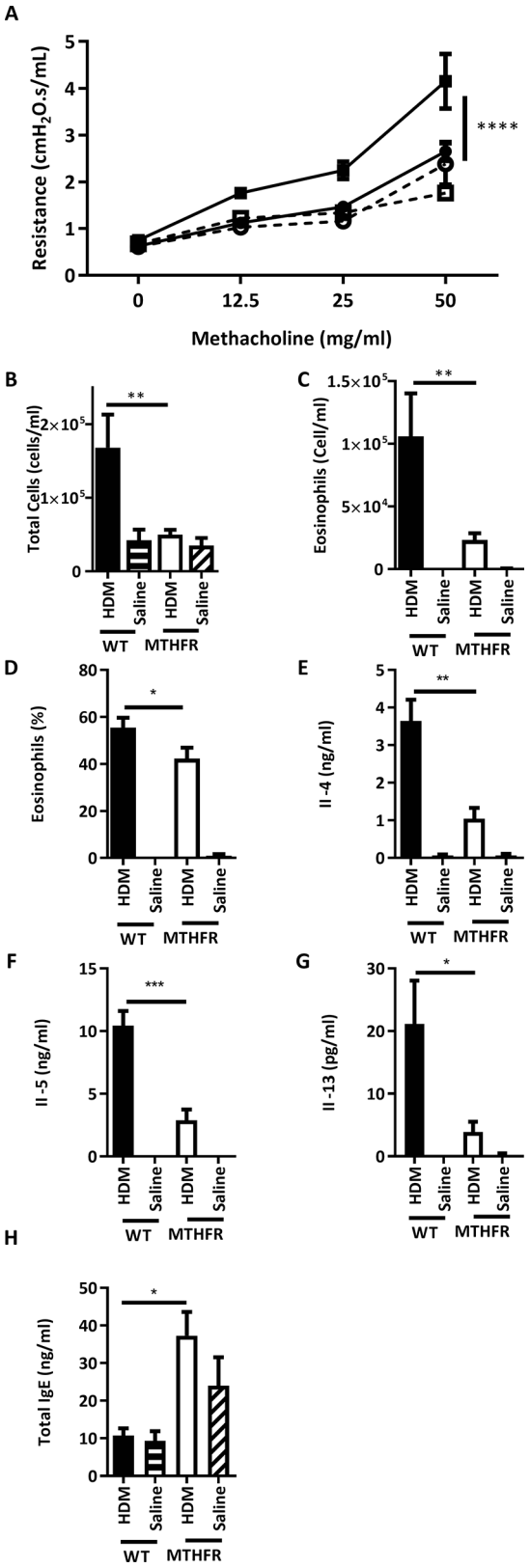

Fig 2. Allergic airway disease was suppressed in C57BL/6$^{Mthfr-/-}$ mice compared to C57BL/6 mice. Loss of Mthfr activity suppressed the severity of HDM-induced allergic airway disease with virtually no changes at baseline. (A)

airway hyperresponsiveness (HDM-treated C57BL/6 solid line closed square, HDM-treated C57BL/6$^{Mthfr-/-}$ solid line closed circle, saline-treated C57BL/6 dashed line open square, and saline-treated C57BL/6$^{Mthfr-/-}$ dashed line open circle), (B) total cells in WLL, and (C) concentration of eosinophils, (D) percentage of eosinophils in the WLL, (E) WLL Il-4 cytokine levels, (F) WLL Il-5 cytokine levels, (G) WLL Il-13 cytokine levels, and (H) total IgE levels in the serum (HDM-treated C57BL/6 black bar, HDM-treated C57BL/6$^{Mthfr-/-}$ white bar, saline-treated C57BL/6 black bar with white dots, and saline-treated C57BL/6$^{Mthfr-/-}$ white bar with black dots, * p-value <0.05, ** p-value <0.01, *** p-value <0.001).

https://doi.org/10.1371/journal.pone.0190916.g002

In summary, loss of Mthfr activity resulted in a suppression of allergic airway disease including the lack of AHR and a reduction of cellular recruitment into the airway without a shift at baseline. However, these mice still developed allergic airway disease characteristics such as increased inflammatory cytokines and eosinophil recruitment.

Gene expression differences between C57BL/6$^{Mthfr-/-}$ and C57BL/6 mice

ANOVA analysis identified 737 genes that are differentially expressed in HDM-treated C57BL/6$^{Mthfr-/-}$ compared to HDM-treated C57BL/6 mice with an adjusted p-value <0.05. 30 of the 737 genes are shared in a similar comparison between saline-treated C57BL/6$^{Mthfr-/-}$ and saline-treated C57BL/6 mice (36). These baseline differences were subtracted from further analyses. Gene clustering by similarity in expression as quantified by the Pearson correlation using average linkage hierarchical clustering identified treatment dependent as well as *Mthfr* status dependent expression patterns (Fig 3).

IPA identified several enriched pathways (S2 Table). As to be expected with C57Bl/6$^{Mthfr-/-}$ mice, a number of biochemical pathways were enriched as loss of Mthfr shifts the balance of other folate forms [18]. There were also a number of immune signaling and developmental pathways identified (S2 Table). S2 Fig is a representative network showing the known interactions of immune genes.

Alterations in C57BL/6$^{Mthfr-/-}$ methylation

Interruption of single carbon metabolism resulted in substantial changes in DNA methylation [9, 16, 17]. Therefore, it is predicted that DNA methylation in C57BL/6$^{Mthfr-/-}$ mice would be altered. Our analysis of 99Mb of the genome selected for areas of high CpG density (Agilent SureSelect) identified a cluster of DMRs around the *Mthfr* gene. Comparing sequence data to known B129 SNP data from the Mouse Genome Informatics database identified a 14Mb region on chromosome 4 in the C57BL/6$^{Mthfr-/-}$ mice as B129 background (S3 Fig). Back-crossing to a pure strain does not result in a 100% congenic strain, thus these results are not unexpected. All results located in this region have been excluded from further discussion.

In the HDM-treated mice, 146 DMRs with an adjusted p-value $\leq$0.10 were identified between C57BL/6$^{Mthfr-/-}$ and C57BL/6 mice (Fig 4A). 32 of the 146 DMRs were shared in a similar comparison between saline-treated C57BL/6$^{Mthfr-/-}$ and saline-treated C57BL/6 mice (247) in terms of physical location or shared nearest gene. These baseline differences were subtracted from further analyses. Of the remaining 114 DMRs (S3 Table), the median length is 90 base pairs (range, 8–719, S3 Table) and were primarily found in gene bodies (intron, exon, 3' untranslated region, or 5' untranslated region; n = 68 or 60%; Fig 4B) and areas distant from CpG islands (>3000 bases from the island; n = 61 or 54%; Fig 4C) with the least amount located in the promoter or within CpG islands. There was a significant enrichment of hypomethylated DMRs (n = 94, p-value = 1.2 x 10^{-12}, S3 Table) in HDM-treated C57BL/6$^{Mthfr-/-}$ mice.

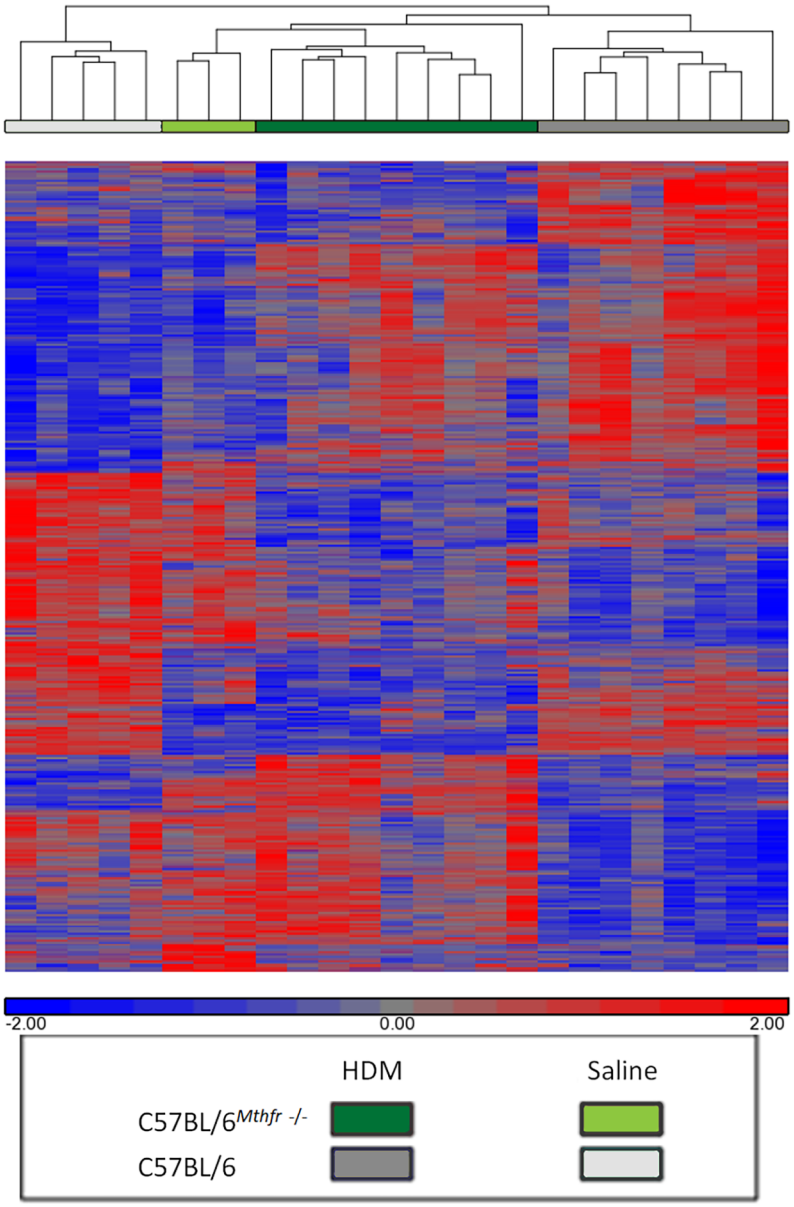

Fig 3. Hierarchal clustering of differentially expressed genes between HDM-treated C57BL/6$^{Mthfr\text{-}/\text{-}}$ and HDM-treated C57BL/6. ANOVA analysis identified 2,588 transcripts that are differentially expressed between the four experimental groups. Gene clustering by similarity in expression as quantified by the Pearson correlation using average linkage hierarchical clustering show groups of genes related to *Mthfr* status as well as treatment dependent clusters.

https://doi.org/10.1371/journal.pone.0190916.g003

Furthermore, we performed subset analyses on methylation clusters within 25kb of asthma related genes as defined by genetic association [30], Ingenuity Pathway Analysis, genes included in the top 10 enriched IPA expression pathways from the study, or overlap of the 3 lists (S4 Table). Statisically significant DMRs (adjusted p-value <0.10) were identified near *Tle4* and *Tnf*; *Scn5a*, *Pde7b*, *Tnf*, and *Rasgrp4*; *Nod2*; and *Tlr9* and *Tnf* respectively (S4 Fig). In summary, our methylation analysis identified that disruption of single carbon metabolism in allergic airway disease leads to a unique methylation profile enriched with hypomethylated DMRs and highlights genes previously associated with disease.

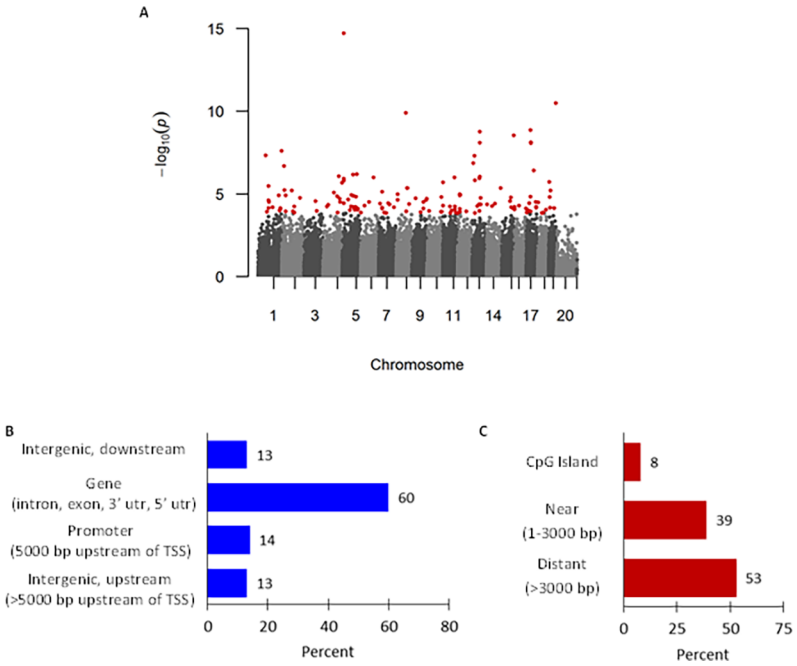

Fig 4. Loss of Mthfr activity in HDM-treated mice was associated with differential DNA methylation. (A) Manhattan plot of the p-values from a weighted beta regression for HDM-treated C57BL/6$^{Mthfr-/-}$ vs. HDM-treated C57BL/6 mice. Each dot represents a p-value for correlating CpG clusters as identified through A-clustering with a minimum of 3 CpGs within a cluster. Red dots denote statistically significant differentially methylated regions (DMRs) after adjustment for multiple testing correction. Genomic distribution of 146 DMRs by relationship to (B) gene and (C) CpG Island.

https://doi.org/10.1371/journal.pone.0190916.g004

Confirmation of expression and methylation analysis

Differentially expressed genes between HDM-treated C57Bl/6$^{Mthfr-/-}$ mice and HDM-treated C57BL/6 mice from the array data were confirmed through qRT-PCR. Genes prioritized for validation were chosen based on statistical significance, fold-change, biological function, and/or proximity to a DMR (Fig 5A). Out of the 8 genes tested, changes in 6 genes were statistically significant (p-value <0.05) and had same directionality and similar magnitude of changes in expression to the array data (Fig 5A).

DMRs were prioritized for validation based on an adjusted p-value <0.10, significant expression differences of nearby genes, and biological function of those genes (Fig 5B). Within the DMRs, percent difference between experimental groups, significant t-test on individual CpGs, and the ability to design primers factored into selecting CpGs for pyrosequencing. DMRs in or near *Rasgrp4*, *Fcer1g*, and *Tle4* were tested. The DMRs validated based on their relation to the methyl sequencing data including statistical difference in the comparison of HDM-treated C57BL/6$^{Mthfr-/-}$ and HDM-treated C57BL/6 mice and similar directional change in percent methylation (Fig 5B).

Methylation-expression quantitative trait region analysis

In relation to expression, there were 7,101 expression probes within 1Mb of the statistically significant DMRs. Of these probes, there was a significant enrichment of canonical anti-correlated methylation-expression relationships (n = 4143, p-value = 1.2 x 10^{-8}); additionally, there was a significant enrichment of transcripts with an uncorrected p-value <0.05 (n = 1,046, p-value = 2.2 x 10^{-16}). In order to more directly measure the relationship between methylation

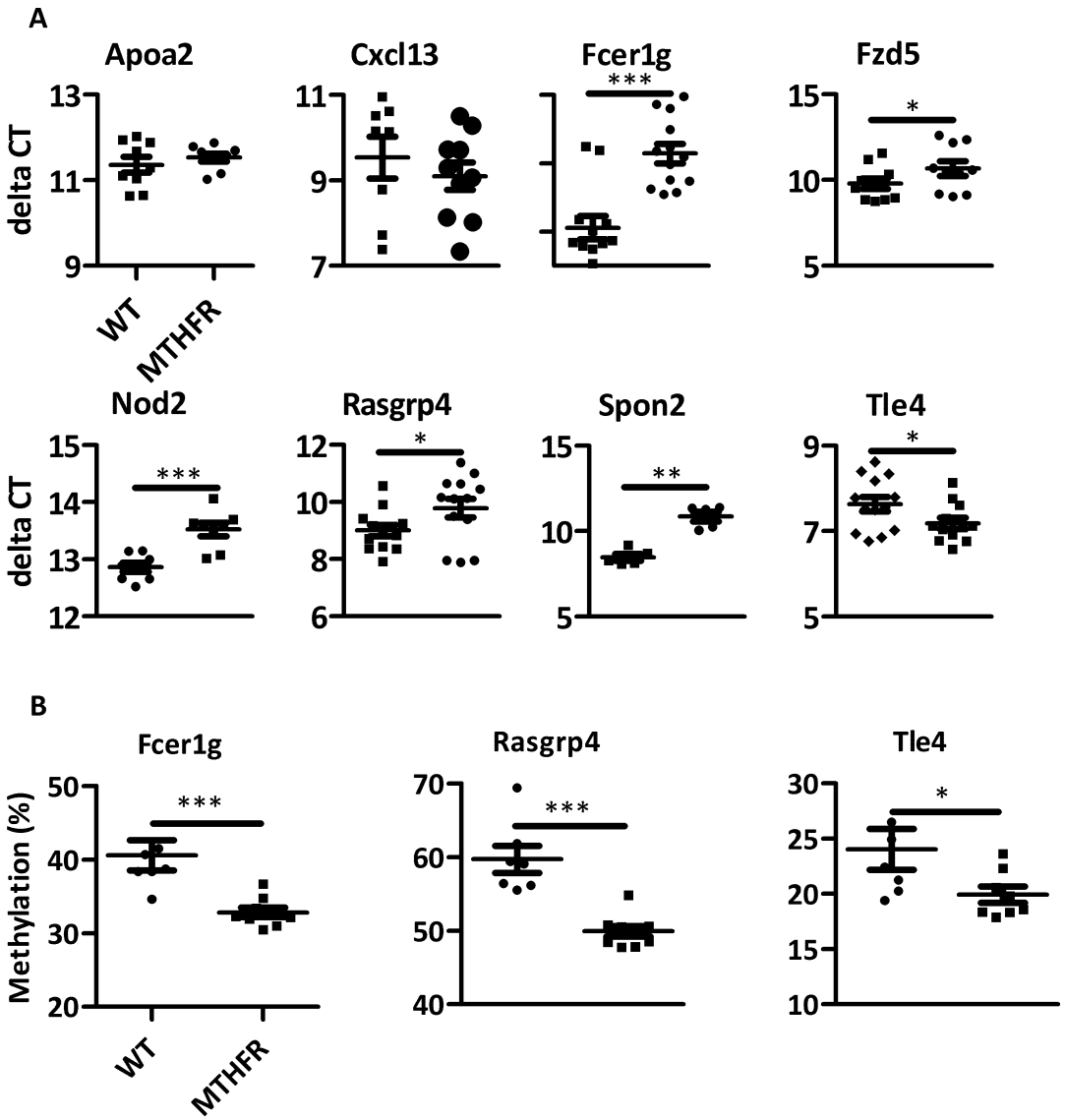

Fig 5. Expression and methylation results were confirmed. (A) 8 differentially expressed genes from the array data were quantified through RT-PCR. 6 out of 8 genes validated. (B) *Rasgrp4*, *Tle4*, and *Fcer1g* DMRs were validated through pyrosequencing. (* p-value <0.05, ** p-value <0.01 *** p-value <0.001).

https://doi.org/10.1371/journal.pone.0190916.g005

and expression, correlation was tested between nominally significant DMRs (n = 6,927) and expression probes within 1 Mb (n = 54,611). 503 significant relationships (corrected p-value <0.05) were identified between expression and methylation data consisting of 354 unique methylation clusters and 491 expression probes (S5 Table). We observed slightly more negative correlations (273), but did not deviate from a normal distribution (p-value = 0.06, S5 Table).

24 pathways were enriched by genes affected by methylation changes, including many involved in inflammatory response (S6 Table). Furthermore, network analysis identified two high-scoring (score >50) networks involved in inflammatory response and development (Fig 6 and S4 Fig). The inflammatory response network contains several genes that have been previously associated with allergic disease, including *Socs3*, *Il9r*, *Icam1*, and *Stat5b*. Additionally, *Etv5* is a transcription factor known to positively regulate *Icam1* [31] and controls Th17

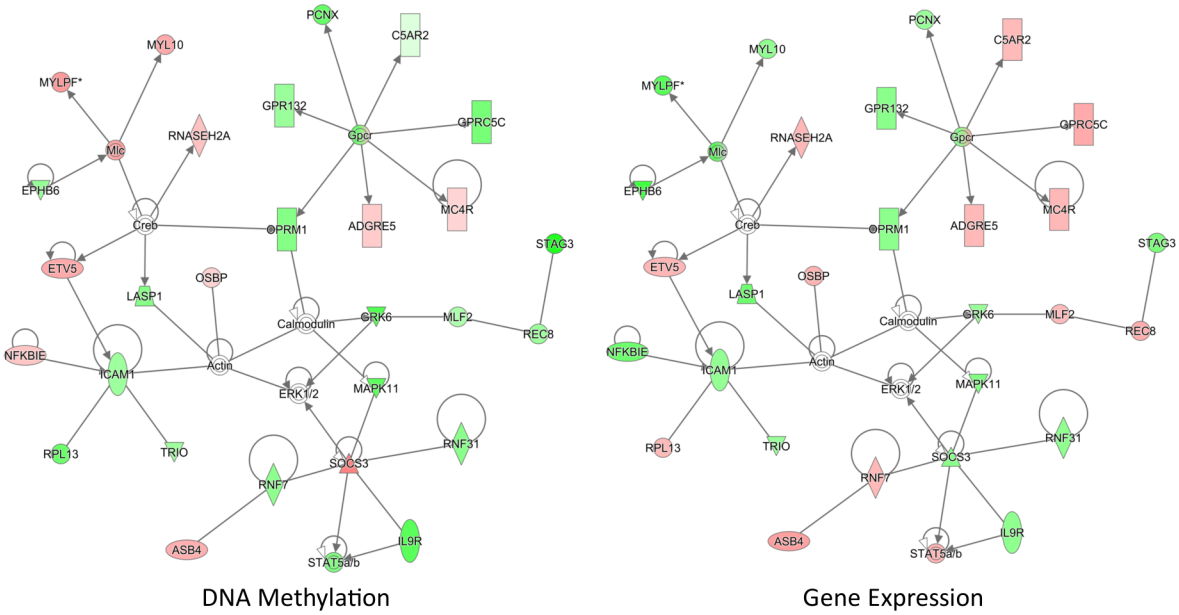

Fig 6. Network of methylation changes directly correlated with transcriptional activity. Methylation changes directly correlated with transcriptional activity. Methylation-expression relationships were measured by beta regression of differentially methylated regions (DMRs, uncorrected p-value <0.05, n = 6,927) associated with HDM-treated C57BL/6$^{Mthfr-/-}$ mice and all expression probes found within 1Mb of each DMR. Ingenuity Pathway Analysis (IPA) on the 503 significant methylation-expression correlations (adjusted p-value <0.05) identified a significant inflammatory response network (score = 52). Green indicates lower methylation or expression and red indicates higher methylation or expression in HDM-treated C57BL/6$^{Mthfr-/-}$ mice. Methylation values are colored based on relative methylation change between HDM-treated C57BL/6$^{Mthfr-/-}$ and HDM-treated C57BL/6 mice; colors of expression values are based on fold change between HDM-treated C57BL/6$^{Mthfr-/-}$ and HDM-treated C57BL/6 mice. Molecule shapes: horizontal oval = transcriptional regulator; vertical oval = transmembrane receptor; diamond = enzyme; up triangle = phosphatase; down triangle = kinase; trapezoid = transporter; circle = other; double circle = group; rectangle = G-protein coupled receptor. This analysis was restricted to only direct relationships. The network score is based on the hypergeometric distribution, and is calculated with the right-tailed Fisher's exact test to identify enrichment of correlated methylated/expressed genes in the network relative to IPA database. The other network with a score greater than 40 is shown in S5 Fig.

https://doi.org/10.1371/journal.pone.0190916.g006

differentiation through the regulation of *Il17a* and *Il17f* expression [32]. These data show that specific methylation changes directly correlate with transcriptional activity of immune related genes.

Betaine supplementation

To confirm the role of Mthfr loss in the attenuation of allergic airway disease, C57BL/6$^{Mthfr-/-}$ and C57BL/6 mice were supplemented with betaine prior to and during HDM treatment. Betaine was selected as it is another co-substrate in the re-methylation of homocysteine and can decrease HCYS to compensate for the loss of 5-methyltetrahydrofolate in the C57BL/6$^{Mthfr-/-}$ mice (refer to Fig 1A). Betaine supplementation resulted in a statistically significant reduction of HCYS and CYSTAT in the serum of C57BL/6$^{Mthfr-/-}$ mice without a change in METH levels (Fig 7A). C57BL/6 mice also demonstrated a decrease in HCYS, but lacked a significant change in CYSTAT or METH (Fig 7A).

Betaine supplemented HDM-treated C57BL/6$^{Mthfr-/-}$ compared to HDM-treated C57BL/6$^{Mthfr-/-}$ mice that were not supplemented with betaine exhibited a significant increase in cellularity and eosinophilia in the WLL without an effect on AHR (Fig 7B–7E). These modified WLL levels are similar to those of HDM-treated C57BL/6 mice that were not supplemented with betaine (Fig 7B–7E). In addition, supplementation in HDM-treated C57BL/6 mice increased the total cells and eosinophils in the WLL compared to values obtained from mice

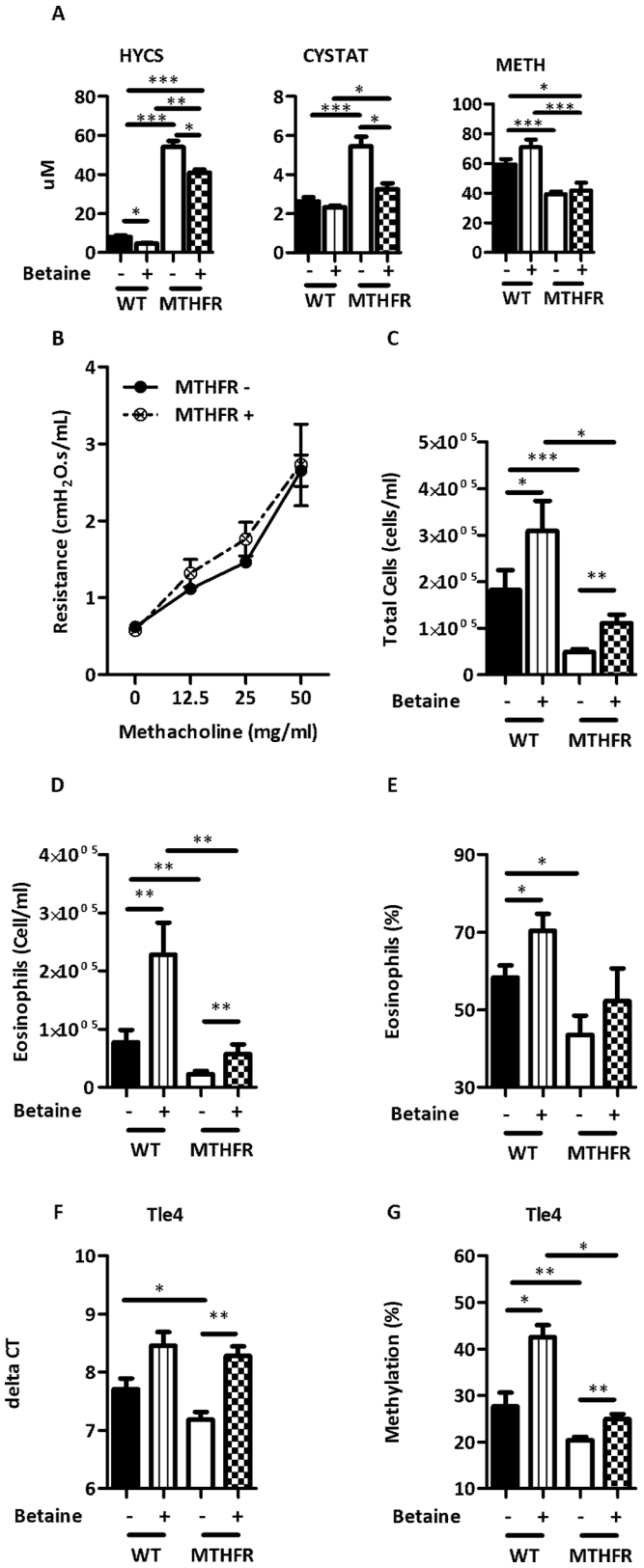

Fig 7. Betaine supplementation exacerbated allergic airway disease. Betaine supplementation affected single carbon metabolites (A) HYCS, CYSTAT, and METH (not supplemented C57BL/6 black bars, supplemented C57BL/6 vertical

striped bars, not supplemented C57Bl/6$^{Mthfr-/-}$ white bars, supplemented C57BL/6$^{Mthfr-/-}$ checkered bars). Betaine supplementation exacerbated the severity of HDM-induced allergic airway disease and abolished the effect of Mthfr loss. (B) Airway hyperresponsiveness (not supplemented HDM-treated C57BL/6$^{Mthfr-/-}$ solid line closed circle, and supplemented C57BL/6$^{Mthfr-/-}$ dashed line open circle and X), and (C) total cells, (D) eosinophils, (E) percentage of eosinophils in WLL. (F) Expression and (G) methylation of *Tle4* is altered by betaine supplementation. (* p-value <0.05, ** p-value <0.01 *** p-value <0.001).

https://doi.org/10.1371/journal.pone.0190916.g007

not supplemented with betaine (Fig 7C–7E). Reversing the AHR phenotype may require longer supplementation with betaine or may not be reversible as lung tissue is fairly differentiated and relatively static, and the underlying molecular drivers of the phenotype could be developmental in origin. Whereas, the immune system is still relatively undifferentiated and plastic at time of supplementation. Supplementation appeared to have no measured effect on saline-treated C57BL/6 mice (data not shown).

In addition to disease phenotype, we assessed expression and methylation levels of *Tle4*; *Tle4* had the strongest evidence for differential methylation and expression in C57BL/6$^{Mthfr-/-}$ mice treated with HDM. Betaine supplementation significantly reduced the expression of *Tle4* in HDM-treated C57BL/6$^{Mthfr-/-}$ mice with a significant increase in DNA methylation. Again, supplementation restored these values to levels comparable to that of HDM-treated C57BL/6 mice not supplemented with betaine. Similarly, HDM-treated C57BL/6 mice demonstrated a statistically significant increase in DNA methylation and a near significant decrease (p-value = 0.06) in expression upon betaine supplementation compared to mice not supplemented with betaine (Fig 7F and 7G).

In summary, the suppressive effect of Mthfr loss was rescued through betaine supplementation and generated a disease phenotype similar to HDM-treated C57BL/6 mice. Moreover, the specific C57BL/6$^{Mthfr-/-}$ expression and methylation pattern of *Tle4* is reversed through supplementation.

Discussion

This study demonstrates that Mthfr and single carbon metabolism may play a role in allergic airway disease. Loss of Mthfr further highlights that disruption of single carbon metabolism leads to molecular changes that reduce Th2 immune responsiveness and allergic airway disease in mice; moreover, we reversed this phenotype through betaine supplementation. These specific findings provide additional understanding of gene environment interactions and epigenetically controlled genes that are relevant in allergic airway disease.

Early immune development is altered in children affected by asthma and allergic disease. This alteration in immune development is characterized by a deficiency of IFNγ production [33, 34], altered innate immunity [35], and deficient Treg networks [36] ultimately leading to uncontrolled Th2 immune responses. Disruption of single carbon metabolism and thus DNA methylation [16, 17] correlates with the severity of Th2 immune responsiveness and allergic airway disease. The availability of methyl donors also associates with an altered T lymphocyte phenotype including skewing of the $CD4^+/CD8^+$ lymphocyte ratio, and production of CC chemokine and IL-4 (unpublished data). Naïve T lymphocyte differentiation into either Th1 or Th2 lineages is regulated through DNA methylation [37, 38], and CD4+ T cells have shown to have folate-sensitive regions [39]. Evaluation of neonates showed a correlation between high maternal folate levels and permissive epigenetic marks at the *GATA3* and *IL-9* loci in CD4+ T cells [40]. Previous *in vitro* studies have observed that hypomethylation in $CD4^+$ T cells leads to increased expression of STAT4 and IFNγ [41] promoting a Th1 response and enhances FoxP3 expression [42] increasing the population of Treg cells. This could explain why we observe a reduced Th2 response in the hypomethylated HDM-treated C57BL/6$^{Mthfr-/-}$ mice.

Also, high levels of methyl donors lead to methylation and repression of *Runx3* (unpublished data), a key regulator of T lymphocyte development and promotor of Th1 cell lineage through the repression of IL-4 [43]. Furthermore, hypomethylation of *Runx3* is nominally significant (p-value = 0.002) in HDM-treated C57BL/6$^{Mthfr\text{-}/\text{-}}$ compared to HDM-treated C57BL/6 mice which would support a more Th1 cell lineage. These findings indicate that Th2 immune responsiveness and development may be modifiable by single carbon metabolism.

Additionally, there are several possible explanations as to why a shift in immune response results from changes in DNA methylation and gene expression. Rasgrp4 is a guanine nucleotide exchange factor that activates Ras [44]. *Rasgrp4* maps to a region on chromosome 7 associated with baseline hyperreactivity in mice, and methacholine hyporesponsive C3H/HeJ mice express a dysfunctional Rasgrp4 protein [45]. *Rasgrp4* is highly expressed in mast cells [46], and loss of Rasgrp4 in mast cells leads to a reduction of FcεRI-mediated degranulation and cytokine production [47]. *Rasgrp4* is differentially methylated and expression is reduced in HDM-treated C57BL/6$^{MTHFR\text{-}/\text{-}}$ mice which correlates with a blunted response upon challenge. Expression changes highlight immune signaling and developmental pathways providing additional evidence for changes in immune function. While the extent of methylation changes is modest, the genes differentially methylated could be master regulators leading to numerous downstream changes. For example, TLE4 is a co-repressor that binds with a number of DNA binding proteins leading to the recruitment of repressor elements. One repressor function of TLE4 is the inhibition of *IFNγ* through epigenetic mechanisms in Th2 cells in order to maintain Th2 identity [48]. TLE4 also alters PAX5, a B cell master regulator, from a transcriptional activator to a repressor [49]. Ingenuity upstream regulator analysis of differentially expressed genes between HDM-treated C57BL/6$^{Mthfr\text{-}/\text{-}}$ and HDM-treated C57BL/6 mice predicted 9 out of the 21 DNA binding proteins that interact with Tle4 to be involved in the changes of expression (S6 Fig). This suggests that changes in key genes could account for numerous downstream changes. Nevertheless, the genes identified in this study are merely associations and further mechanistic work is needed to show direct relationship with the underlying biology that alters disease severity.

Polymorphisms of *MTHFR* appear to modulate a number of phenotypes. The C677T *MTHFR* SNP is common in the human population and affects global methylation [18]. It has been postulated that the C677T SNP may have immune-protective properties [50]. A study of hepatitis B virus (HBV) infection in a West African population showed that the T allele independently associated with the persistence of detectable anti-HBs antibodies and a reduced level of HBV DNA [51]. In another study, Mthfr deficient mice compared to wild-type littermates responded better to mouse cytomegalovirus infection in terms of early control of cytokine secretion, decreased viral titer, and spleen immune cell preservation [50]. Furthermore, a mouse model of cerebral malaria showed that *Mthfr* overexpression had worse survival rates compared to wild-type mice while *Mthfr* deficient mice survived longer [52]. Our results further demonstrate that loss of Mthfr function results in an altered immune response in a HDM model of allergic airway disease.

A limitation in this study is that the methylation experiment was completed on whole lung tissue with an admixture of cells. Cell type specific expression and methylation patterns increases variance in the analysis creating a higher threshold for discovery. Alternatively, the small number of methylation changes suggests that other regulatory mechanisms could be contributing to the shift in phenotype including histone modifications, non-coding RNAs, and/or protein modifications.

This is the first work to be published that has examined the role of Mthfr in an animal model of allergic airway disease. While the severe deficiency of Mthfr found in C57BL/6$^{Mthfr\text{-}/\text{-}}$ mice is not common in the general population, our results may prove relevant to asthma in humans. Our approach in Mthfr deficient mice has identified genes that are regulated in disease and responsive to gene environment interactions. Furthermore, it highlights that asthma

risk genes can be affected through both genetic and environmental mechanisms. For example, *TLE4* was previously associated with asthma in a GWAS with the associated SNP lying upstream of the gene likely affecting its regulation [53]. Here we have found an association between *Tle4* and allergic airway disease in mice through a change in DNA methylation suggesting that different paths likely lead to the development of allergic airway disease in mice.

Supporting information

S1 Appendix. Supplemental figure description.
(DOCX)

S1 Fig. INFγ ELISA.
(TIF)

S2 Fig. Expression network of immune signaling and developmental pathways.
(TIF)

S3 Fig. B129 SNP calls.
(TIF)

S4 Fig. Top 10 enriched IPA expression pathways.
(TIF)

S5 Fig. Expression and methylation development network.
(TIF)

S6 Fig. Tle4 interaction network.
(TIF)

S1 Table. Agilent SureSelect methyl sequencing summary.
(XLSX)

S2 Table. IPA enriched pathways from differentially expressed genes between the HDM-treated groups.
(XLSX)

S3 Table. Statistically significant DMRs in HDM-treated C57BL/6$^{MTHFR-/-}$ and C57BL/6 mice.
(XLSX)

S4 Table. DMR subset analysis of gene lists.
(XLSX)

S5 Table. Significant methylation-expression correlations within 1MB.
(XLSX)

S6 Table. Pathways of significant methylation-expression correlations within 1MB.
(XLSX)

S7 Table. Pyrosequencing primers.
(XLSX)

Author Contributions

Conceptualization: Kenneth R. Eyring, Kenneth N. Maclean, Sally P. Stabler, Ivana V. Yang, David A. Schwartz.

Data curation: Kenneth R. Eyring.

Formal analysis: Kenneth R. Eyring, Brent S. Pedersen.

Funding acquisition: Ivana V. Yang, David A. Schwartz.

Investigation: Kenneth R. Eyring.

Methodology: Kenneth R. Eyring, Brent S. Pedersen, Kenneth N. Maclean, Sally P. Stabler, Ivana V. Yang, David A. Schwartz.

Resources: Brent S. Pedersen, Kenneth N. Maclean, Sally P. Stabler, Ivana V. Yang, David A. Schwartz.

Supervision: Kenneth N. Maclean, Sally P. Stabler, Ivana V. Yang, David A. Schwartz.

Writing – original draft: Kenneth R. Eyring.

Writing – review & editing: Kenneth R. Eyring, Brent S. Pedersen, Kenneth N. Maclean, Sally P. Stabler, Ivana V. Yang, David A. Schwartz.

References

1. Bousquet J, Ndiaye M, Ait-Khaled N, Annesi-Maesano I, Vignola AM. Management of chronic respiratory and allergic diseases in developing countries. Focus on sub-Saharan Africa. Allergy. 2003; 58 (4):265–83. PMID: 12708972
2. Burney P. The changing prevalence of asthma? Thorax. 2002; 57 Suppl 2:II36–II9.
3. Kit BK, Simon AE, Ogden CL, Akinbami LJ. Trends in preventive asthma medication use among children and adolescents, 1988–2008. Pediatrics. 2012; 129(1):62–9. https://doi.org/10.1542/peds.2011-1513 PMID: 22144697
4. Dunstan JA, Mori TA, Barden A, Beilin LJ, Taylor AL, Holt PG, et al. Fish oil supplementation in pregnancy modifies neonatal allergen-specific immune responses and clinical outcomes in infants at high risk of atopy: a randomized, controlled trial. The Journal of allergy and clinical immunology. 2003; 112 (6):1178–84. https://doi.org/10.1016/j.jaci.2003.09.009 PMID: 14657879
5. Fitzsimon N, Fallon U, O'Mahony D, Loftus BG, Bury G, Murphy AW, et al. Mothers' dietary patterns during pregnancy and risk of asthma symptoms in children at 3 years. Ir Med J. 2007; 100(8):suppl 27–32.
6. Samet JM, Lambert WE. Epidemiologic approaches for assessing health risks from complex mixtures in indoor air. Environmental health perspectives. 1991; 95:71–4. PMID: 1821382
7. Sporik R, Holgate ST, Platts-Mills TA, Cogswell JJ. Exposure to house-dust mite allergen (Der p I) and the development of asthma in childhood. A prospective study. The New England journal of medicine. 1990; 323(8):502–7. https://doi.org/10.1056/NEJM199008233230802 PMID: 2377175
8. Breton CV, Byun HM, Wenten M, Pan F, Yang A, Gilliland FD. Prenatal tobacco smoke exposure affects global and gene-specific DNA methylation. American journal of respiratory and critical care medicine. 2009; 180(5):462–7. https://doi.org/10.1164/rccm.200901-0135OC PMID: 19498054
9. Hollingsworth JW, Maruoka S, Boon K, Garantziotis S, Li Z, Tomfohr J, et al. In utero supplementation with methyl donors enhances allergic airway disease in mice. J Clin Invest. 2008; 118(10):3462–9. https://doi.org/10.1172/JCI34378 PMID: 18802477
10. Schaub B, Liu J, Hoppler S, Schleich I, Huehn J, Olek S, et al. Maternal farm exposure modulates neonatal immune mechanisms through regulatory T cells. The Journal of allergy and clinical immunology. 2009; 123(4):774–82 e5. https://doi.org/10.1016/j.jaci.2009.01.056 PMID: 19348917
11. Vuillermin PJ, Ponsonby AL, Saffery R, Tang ML, Ellis JA, Sly P, et al. Microbial exposure, interferon gamma gene demethylation in naive T-cells, and the risk of allergic disease. Allergy. 2009; 64(3):348–53. https://doi.org/10.1111/j.1398-9995.2009.01970.x PMID: 19210359
12. Kabesch M. Early origins of asthma (and allergy). Mol Cell Pediatr. 2016; 3(1):31. https://doi.org/10.1186/s40348-016-0056-4 PMID: 27510897
13. Harb H, Alashkar Alhamwe B, Garn H, Renz H, Potaczek DP. Recent developments in epigenetics of pediatric asthma. Curr Opin Pediatr. 2016; 28(6):754–63. https://doi.org/10.1097/MOP.0000000000000424 PMID: 27662207

14. Allis CD, Jenuwein T, Reinberg D. Epigenetics. Cold Spring Harbor, N.Y.: Cold Spring Harbor Laboratory Press; 2007. x, 502 p. p.

15. Waterland RA, Michels KB. Epigenetic epidemiology of the developmental origins hypothesis. Annu Rev Nutr. 2007; 27:363–88. https://doi.org/10.1146/annurev.nutr.27.061406.093705 PMID: 17465856

16. Wainfan E, Dizik M, Stender M, Christman JK. Rapid appearance of hypomethylated DNA in livers of rats fed cancer-promoting, methyl-deficient diets. Cancer research. 1989; 49(15):4094–7. PMID: 2743304

17. Wilson MJ, Shivapurkar N, Poirier LA. Hypomethylation of hepatic nuclear DNA in rats fed with a carcinogenic methyl-deficient diet. The Biochemical journal. 1984; 218(3):987–90. PMID: 6721844

18. Friso S, Choi SW, Girelli D, Mason JB, Dolnikowski GG, Bagley PJ, et al. A common mutation in the 5,10-methylenetetrahydrofolate reductase gene affects genomic DNA methylation through an interaction with folate status. Proceedings of the National Academy of Sciences of the United States of America. 2002; 99(8):5606–11. https://doi.org/10.1073/pnas.062066299 PMID: 11929966

19. Thuesen BH, Husemoen LL, Fenger M, Linneberg A. Lack of association between the MTHFR (C677T) polymorphism and atopic disease. The clinical respiratory journal. 2009; 3(2):102–8. https://doi.org/10.1111/j.1752-699X.2009.00128.x PMID: 20298385

20. Thuesen BH, Husemoen LL, Ovesen L, Jorgensen T, Fenger M, Linneberg A. Lifestyle and genetic determinants of folate and vitamin B12 levels in a general adult population. The British journal of nutrition. 2010; 103(8):1195–204. https://doi.org/10.1017/S0007114509992947 PMID: 19968891

21. Zou CC, Tang LF, Jiang MZ, Zhao ZY, Hirokazu T, Mitsufumi M. [Methylenetetrahydrofolate reductase [correction of reducatase] polymorphism and asthma]. Zhonghua jie he he hu xi za zhi = Zhonghua jiehe he huxi zazhi = Chinese journal of tuberculosis and respiratory diseases. 2003; 26(3):161–4. PMID: 12816682

22. van der Valk RJ, Kiefte-de Jong JC, Sonnenschein-van der Voort AM, Duijts L, Hafkamp-de Groen E, Moll HA, et al. Neonatal folate, homocysteine, vitamin B12 levels and methylenetetrahydrofolate reductase variants in childhood asthma and eczema. Allergy. 2013; 68(6):788–95. https://doi.org/10.1111/all.12146 PMID: 23692062

23. Delaney C, Hoeltzel M, Garg SK, Warner R, Johnson K, Yung R. Maternal micronutrient supplementation suppresses T cell chemokine receptor expression and function in F1 mice. The Journal of nutrition. 2012; 142(7):1329–35. https://doi.org/10.3945/jn.111.155903 PMID: 22649261

24. Mehta AK, Singh BP, Arora N, Gaur SN. Choline attenuates immune inflammation and suppresses oxidative stress in patients with asthma. Immunobiology. 2010; 215(7):527–34. https://doi.org/10.1016/j.imbio.2009.09.004 PMID: 19897276

25. Knock E, Deng L, Wu Q, Lawrance AK, Wang XL, Rozen R. Strain differences in mice highlight the role of DNA damage in neoplasia induced by low dietary folate. The Journal of nutrition. 2008; 138(4):653–8. PMID: 18356316

26. Maclean KN, Jiang H, Greiner LS, Allen RH, Stabler SP. Long-term betaine therapy in a murine model of cystathionine beta-synthase deficient homocystinuria: decreased efficacy over time reveals a significant threshold effect between elevated homocysteine and thrombotic risk. Molecular genetics and metabolism. 2012; 105(3):395–403. https://doi.org/10.1016/j.ymgme.2011.11.190 PMID: 22192524

27. Pedersen BS, Eyring K, De S, Yang IV, Schwartz DA. Fast and accurate alignment of long bisulfite-seq reads. ArXiv e-prints [Internet]. 2014 January 1, 2014; 1401:[1129 p.]. Available from: http://adsabs.harvard.edu/abs/2014arXiv1401.1129P.

28. Sofer T, Schifano ED, Hoppin JA, Hou L, Baccarelli AA. A-clustering: a novel method for the detection of co-regulated methylation regions, and regions associated with exposure. Bioinformatics. 2013; 29(22):2884–91. https://doi.org/10.1093/bioinformatics/btt498 PMID: 23990415

29. Klipper-Aurbach Y, Wasserman M, Braunspiegel-Weintrob N, Borstein D, Peleg S, Assa S, et al. Mathematical formulae for the prediction of the residual beta cell function during the first two years of disease in children and adolescents with insulin-dependent diabetes mellitus. Medical hypotheses. 1995; 45(5):486–90. PMID: 8748093

30. DeWan AT, Egan KB, Hellenbrand K, Sorrentino K, Pizzoferrato N, Walsh KM, et al. Whole-exome sequencing of a pedigree segregating asthma. BMC medical genetics. 2012; 13:95. https://doi.org/10.1186/1471-2350-13-95 PMID: 23046476

31. de Launoit Y, Audette M, Pelczar H, Plaza S, Baert JL. The transcription of the intercellular adhesion molecule-1 is regulated by Ets transcription factors. Oncogene. 1998; 16(16):2065–73. https://doi.org/10.1038/sj.onc.1201726 PMID: 9572487

32. Pham D, Sehra S, Sun X, Kaplan MH. The transcription factor Etv5 controls TH17 cell development and allergic airway inflammation. The Journal of allergy and clinical immunology. 2014; 134(1):204–14. https://doi.org/10.1016/j.jaci.2013.12.021 PMID: 24486067

33. Martinez FD, Stern DA, Wright AL, Holberg CJ, Taussig LM, Halonen M. Association of interleukin-2 and interferon-gamma production by blood mononuclear cells in infancy with parental allergy skin tests and with subsequent development of atopy. The Journal of allergy and clinical immunology. 1995; 96(5 Pt 1):652–60.

34. Tang ML, Kemp AS, Thorburn J, Hill DJ. Reduced interferon-gamma secretion in neonates and subsequent atopy. Lancet. 1994; 344(8928):983–5. PMID: 7934430

35. Yerkovich ST, Wikstrom ME, Suriyaarachchi D, Prescott SL, Upham JW, Holt PG. Postnatal development of monocyte cytokine responses to bacterial lipopolysaccharide. Pediatr Res. 2007; 62(5):547–52. https://doi.org/10.1203/PDR.0b013e3181568105 PMID: 17805207

36. Smith M, Tourigny MR, Noakes P, Thornton CA, Tulic MK, Prescott SL. Children with egg allergy have evidence of reduced neonatal CD4(+)CD25(+)CD127(lo/-) regulatory T cell function. The Journal of allergy and clinical immunology. 2008; 121(6):1460–6, 6 e1-7. https://doi.org/10.1016/j.jaci.2008.03.025 PMID: 18455222

37. Kwon NH, Kim JS, Lee JY, Oh MJ, Choi DC. DNA methylation and the expression of IL-4 and IFN-gamma promoter genes in patients with bronchial asthma. Journal of clinical immunology. 2008; 28(2):139–46. https://doi.org/10.1007/s10875-007-9148-1 PMID: 18004650

38. Williams CL, Schilling MM, Cho SH, Lee K, Wei M, Aditi, et al. STAT4 and T-bet are required for the plasticity of IFN-gamma expression across Th2 ontogeny and influence changes in Ifng promoter DNA methylation. J Immunol. 2013; 191(2):678–87. https://doi.org/10.4049/jimmunol.1203360 PMID: 23761633

39. Amarasekera M, Martino D, Ashley S, Harb H, Kesper D, Strickland D, et al. Genome-wide DNA methylation profiling identifies a folate-sensitive region of differential methylation upstream of ZFP57-imprinting regulator in humans. FASEB J. 2014; 28(9):4068–76. https://doi.org/10.1096/fj.13-249029 PMID: 24891518

40. Harb H, Amarasekera M, Ashley S, Tulic MK, Pfefferle PI, Potaczek DP, et al. Epigenetic Regulation in Early Childhood: A Miniaturized and Validated Method to Assess Histone Acetylation. Int Arch Allergy Immunol. 2015; 168(3):173–81. https://doi.org/10.1159/000442158 PMID: 26789836

41. Shin HJ, Park HY, Jeong SJ, Park HW, Kim YK, Cho SH, et al. STAT4 expression in human T cells is regulated by DNA methylation but not by promoter polymorphism. J Immunol. 2005; 175(11):7143–50. PMID: 16301617

42. Kim HP, Leonard WJ. CREB/ATF-dependent T cell receptor-induced FoxP3 gene expression: a role for DNA methylation. The Journal of experimental medicine. 2007; 204(7):1543–51. https://doi.org/10.1084/jem.20070109 PMID: 17591856

43. Djuretic IM, Levanon D, Negreanu V, Groner Y, Rao A, Ansel KM. Transcription factors T-bet and Runx3 cooperate to activate Ifng and silence Il4 in T helper type 1 cells. Nature immunology. 2007; 8(2):145–53. https://doi.org/10.1038/ni1424 PMID: 17195845

44. Ebinu JO, Bottorff DA, Chan EY, Stang SL, Dunn RJ, Stone JC. RasGRP, a Ras guanyl nucleotide-releasing protein with calcium- and diacylglycerol-binding motifs. Science. 1998; 280(5366):1082–6. PMID: 9582122

45. Stevens RL, Morokawa N, Wang J, Krilis SA. RasGRP4 in mast cell signalling and disease susceptibility. Novartis Foundation symposium. 2005; 271:54–68; discussion -77, 95–9. PMID: 16605128

46. Li L, Yang Y, Stevens RL. Cloning of rat Ras guanine nucleotide releasing protein 4, and evaluation of its expression in rat mast cells and their bone marrow progenitors. Molecular immunology. 2002; 38(16–18):1283–8. PMID: 12217396

47. Zhu M, Fuller DM, Zhang W. The role of Ras guanine nucleotide releasing protein 4 in Fc epsilonRI-mediated signaling, mast cell function, and T cell development. The Journal of biological chemistry. 2012; 287(11):8135–43. https://doi.org/10.1074/jbc.M111.320580 PMID: 22262848

48. Bandyopadhyay S, Valdor R, Macian F. Tle4 regulates epigenetic silencing of gamma interferon expression during effector T helper cell tolerance. Molecular and cellular biology. 2014; 34(2):233–45. https://doi.org/10.1128/MCB.00902-13 PMID: 24190972

49. Patel SR, Bhumbra SS, Paknikar RS, Dressler GR. Epigenetic mechanisms of Groucho/Grg/TLE mediated transcriptional repression. Molecular cell. 2012; 45(2):185–95. https://doi.org/10.1016/j.molcel.2011.11.007 PMID: 22169276

50. Fodil-Cornu N, Kozij N, Wu Q, Rozen R, Vidal SM. Methylenetetrahydrofolate reductase (MTHFR) deficiency enhances resistance against cytomegalovirus infection. Genes and immunity. 2009; 10(7):662–6. https://doi.org/10.1038/gene.2009.50 PMID: 19609317

51. Toniutto P, Fabris C, Falleti E, Cussigh A, Fontanini E, Bitetto D, et al. Methylenetetrahydrofolate reductase C677T polymorphism and liver fibrosis progression in patients with recurrent hepatitis C. Liver international: official journal of the International Association for the Study of the Liver. 2008; 28(2):257–63.

52. Meadows DN, Pyzik M, Wu Q, Torre S, Gros P, Vidal SM, et al. Increased resistance to malaria in mice with methylenetetrahydrofolate reductase (Mthfr) deficiency suggests a mechanism for selection of the MTHFR 677C>T (c.665C>T) variant. Human mutation. 2014; 35(5):594–600. https://doi.org/10.1002/humu.22533 PMID: 24616178

53. Hancock DB, Romieu I, Shi M, Sienra-Monge JJ, Wu H, Chiu GY, et al. Genome-wide association study implicates chromosome 9q21.31 as a susceptibility locus for asthma in mexican children. PLoS genetics. 2009; 5(8):e1000623. https://doi.org/10.1371/journal.pgen.1000623 PMID: 19714205

Allergic Airway Disease is Dependent on Methylene-Tetrahydrofolate Reductase

Kenneth R Eyring, Brent S. Pedersen, Kenneth N. Maclean, Sally P. Stabler, Ivana V. Yang, David A. Schwartz

Online Data Supplement

Supplemental Figure S1: Inf-γ was observed in saline treated mice and was reduced or lost in HDM-treated mice indicating a shift toward Th2 upon HDM-treatment.

Supplemental Figure S2: A representative molecular network from IPA of differently expressed genes. Network analysis was performed using only direct interactions and a minimum network score of 20. Legend: genes are colored red (up-regulated) or green (down-regulated), horizontal ellipse = transcriptional regulator, square = cytokine, double circle = group/complex, upside down triangle = kinase, vertical diamond = enzyme, vertical rectangle = G-protein coupled receptor

Supplemental Figure S3: C57BL/6$^{Mthfr-/-}$ sequence was compared against know B129 SNPs from the Mouse Genome Informatics database. Each dot represents a SNP plotted by its chromosomal location on the x-axis and the percentage of reads that matched on the y-axis.

Supplemental Figure S4: Subset analyses on methylation clusters between C57BL/6$^{Mthfr-/-}$ and C57BL/6 mice located within 25kb of asthma related genes as defined by genetic association (5), Ingenuity Pathway Analysis, genes included in the top 10 enriched IPA expression pathways from the study, or overlap of the 3 lists were performed. Statisically significant DMRs (adjusted p-value <0.10) were identified near *Tle4* and *Tnf*; *Scn5a*, *Pde7b*, *Tnf*, and *Rasgrp4*; *Nod2*; and *Tlr9* and *Tnf* respectively

Supplemental Figure S5: Methylation changes directly correlate with transcriptional activity. Methylation-expression relationships were measured by beta regression of differentially methylated regions (DMRs, uncorrected p-value <0.05, n = 6,927) associated with HDM-treated C57BL/6$^{Mthfr-/-}$ mice and all expression probes found within 1Mb of each DMR. Ingenuity

Pathway Analysis (IPA) on the 503 significant methylation-expression correlations (adjusted p-value <0.05) identified a significant inflammatory response network (score = 52). Green indicates lower methylation or expression and red indicates higher methylation or expression in HDM-treated C57BL/6$^{Mthfr-/-}$ mice. Methylation values are colored based on relative methylation change between HDM-treated C57BL/6$^{Mthfr-/-}$ and HDM-treated C57BL/6 mice; colors of expression values are based on fold change between HDM-treated C57BL/6$^{Mthfr-/-}$ and HDM-treated C57BL/6 mice. Molecule shapes: horizontal oval = transcriptional regulator; vertical oval = transmembrane receptor; diamond = enzyme; up triangle = phosphatase; down triangle = kinase; trapezoid = transporter; circle = other; double circle = group; rectangle = G-protein coupled receptor. This analysis was restricted to only direct relationships. The network score is based on the hypergeometric distribution, and is calculated with the right-tailed Fisher's exact test to identify enrichment of correlated methylated/expressed genes in the network relative to IPA database.

Supplemental Figure S6: Ingenuity upstream analysis on differentially expressed genes between HDM-treated C57BL/6$^{Mthfr-/-}$ and HDM-treated C57BL/6 mice predicted 9 (circled in red) of the 21 DNA binding proteins that interact with TLE4 to be involved in changes of expression.

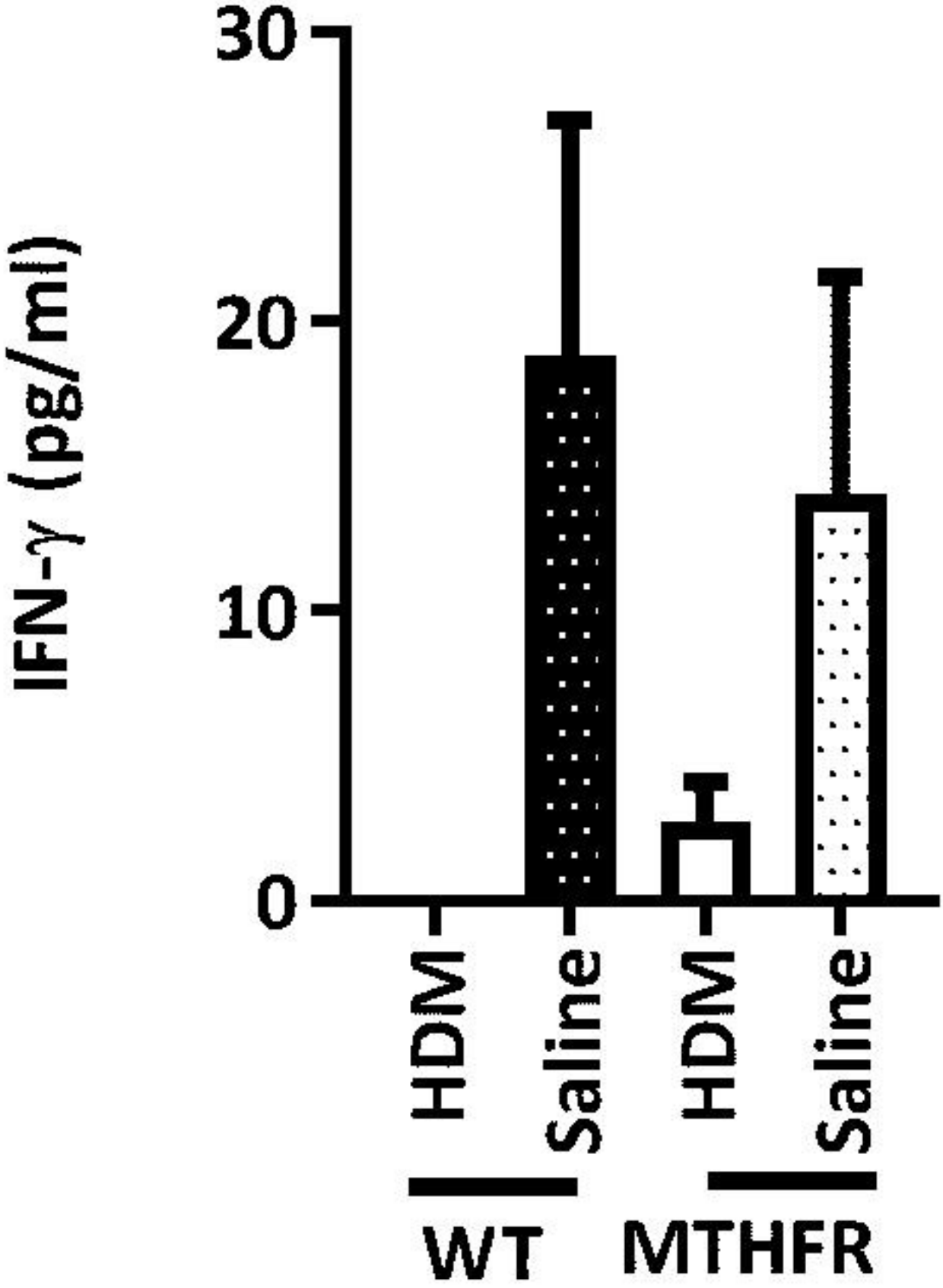
IFN-γ (pg/ml)
30
20
10
0
HDM
Saline
HDM
Saline
WT
MTHFR

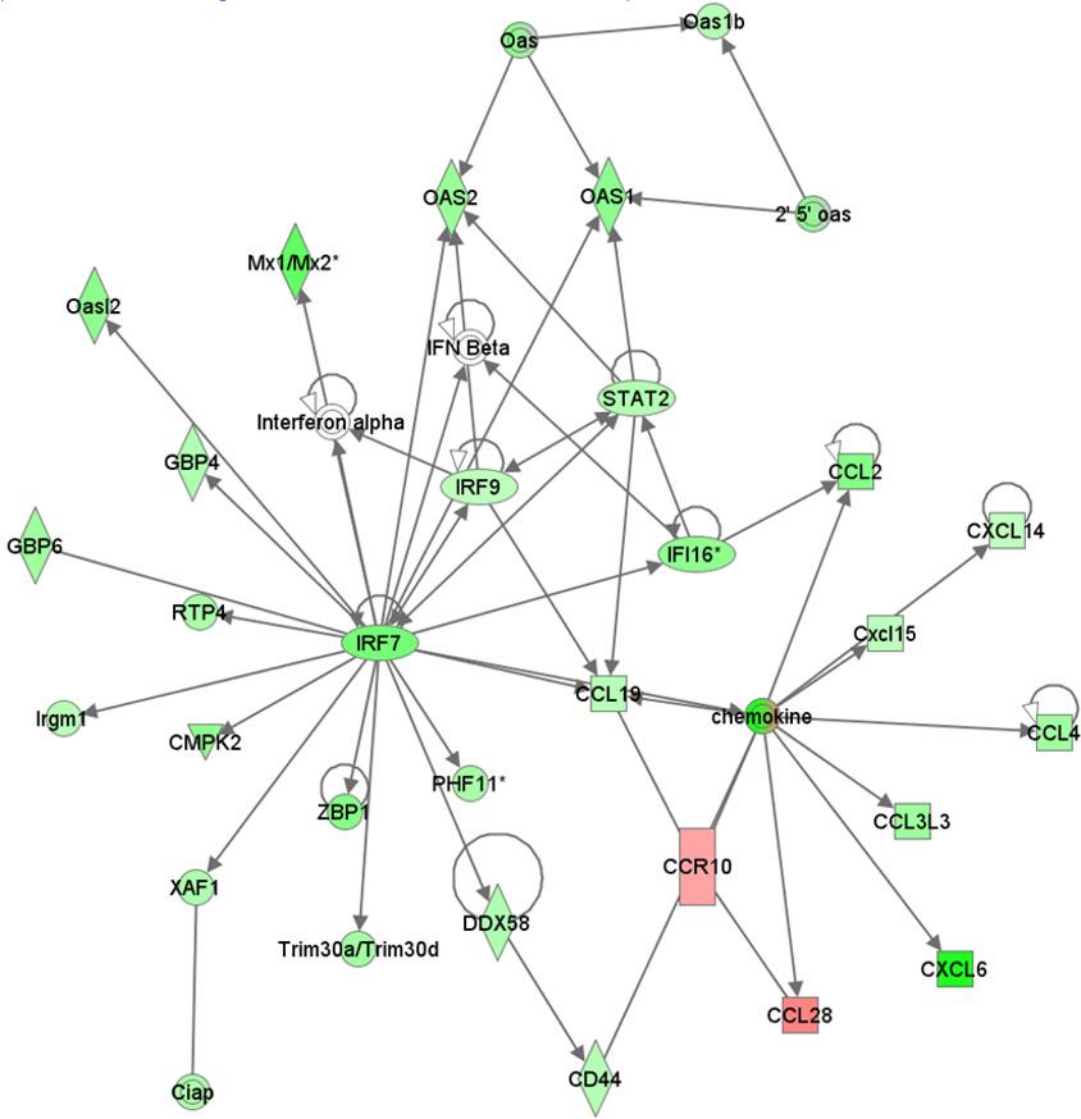
Oas
Oas1b
OAS2
OAS1
2' 5' oas
Mx1/Mx2*
Oasl2
IFN Beta
STAT2
Interferon alpha
GBP4
IRF9
CCL2
GBP6
IFI16*
CXCL14
RTP4
IRF7
Cxcl15
CCL19
Irgm1
chemokine
CCL4
CMPK2
PHF11*
ZBP1
CCL3L3
CCR10
XAF1
DDX58
Trim30a/Trim30d
CXCL6
CCL28
CD44
Ciap

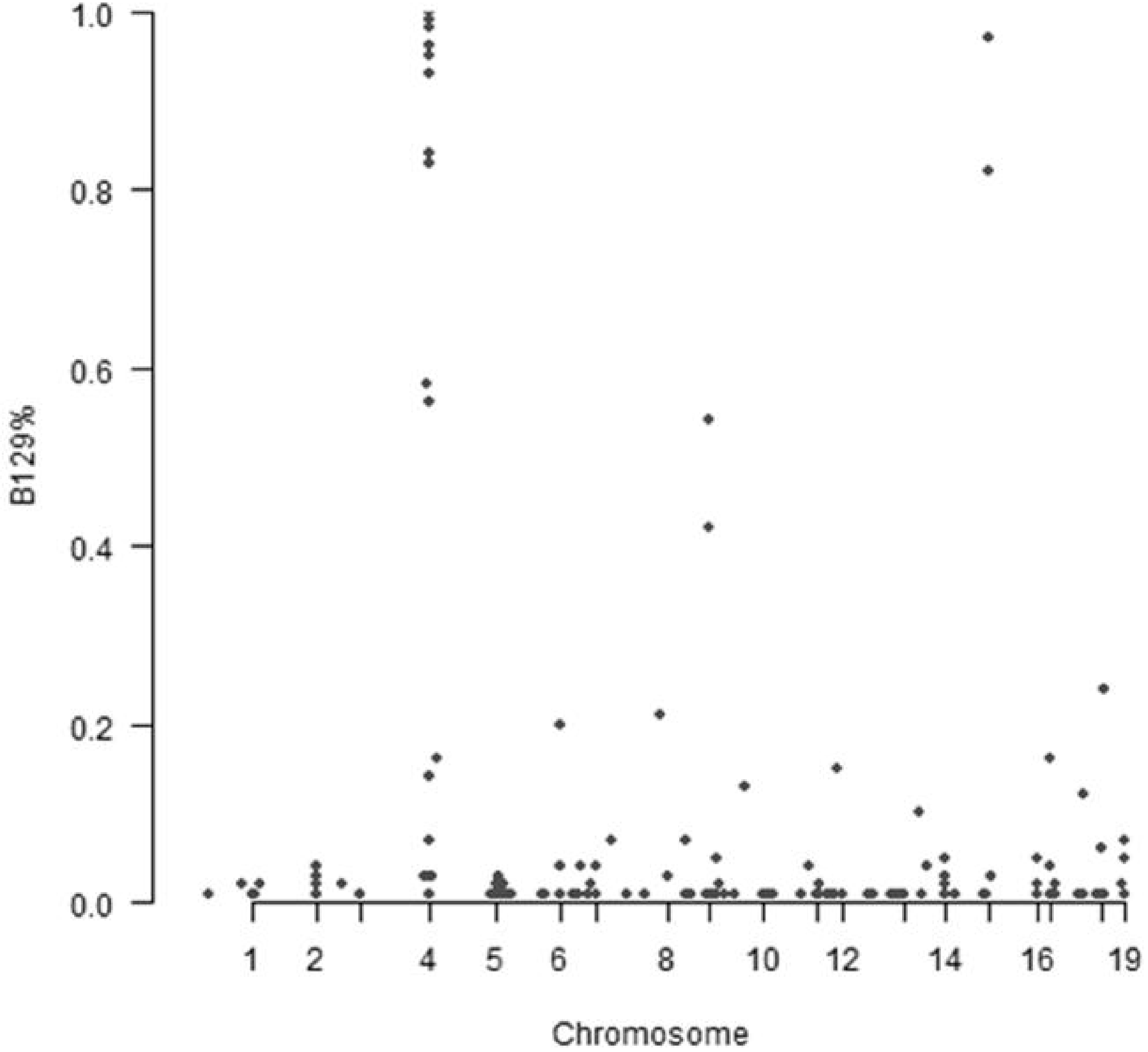
1.0
0.8
0.6
0.4
0.2
0.0
B129%
1
2
4
5
6
8
10
12
14
16
19
Chromosome

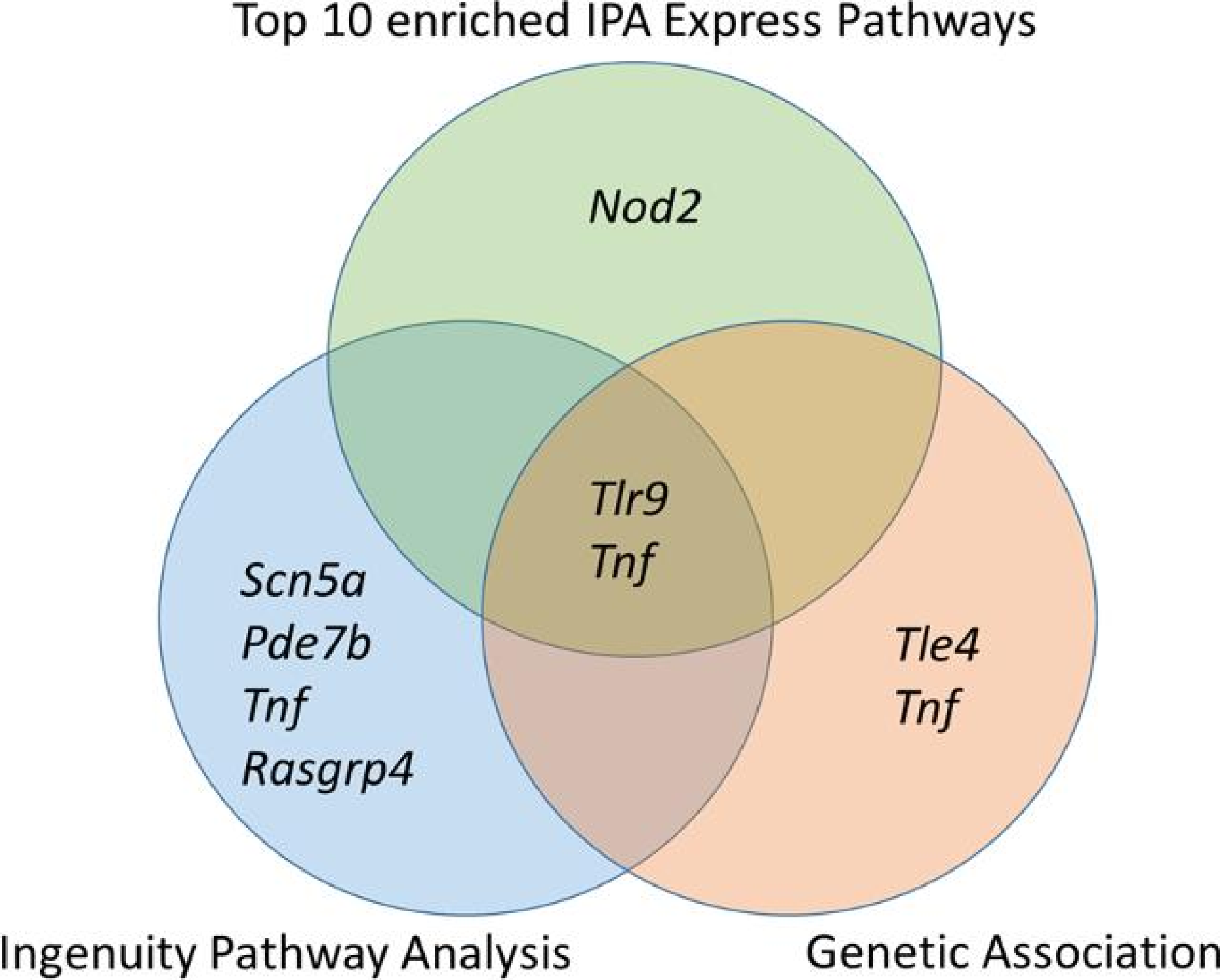
Top 10 enriched IPA Express Pathways
Nod2
Tlr9
Tnf
Scn5a
Pde7b
Tnf
Rasgrp4
Tle4
Tnf
Ingenuity Pathway Analysis
Genetic Association

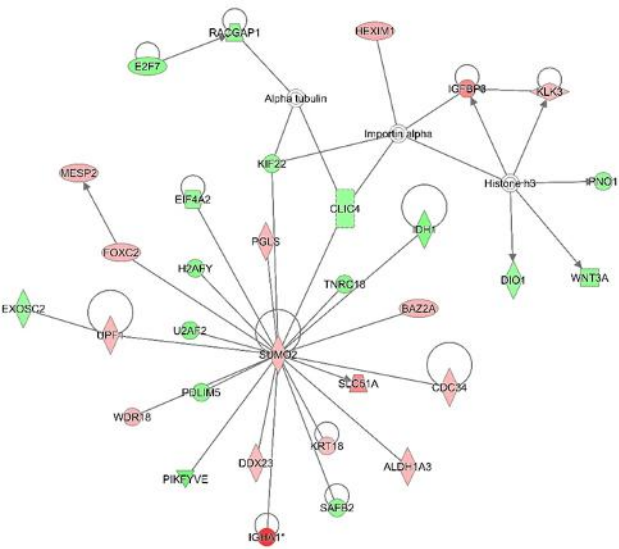

DNA Methylation

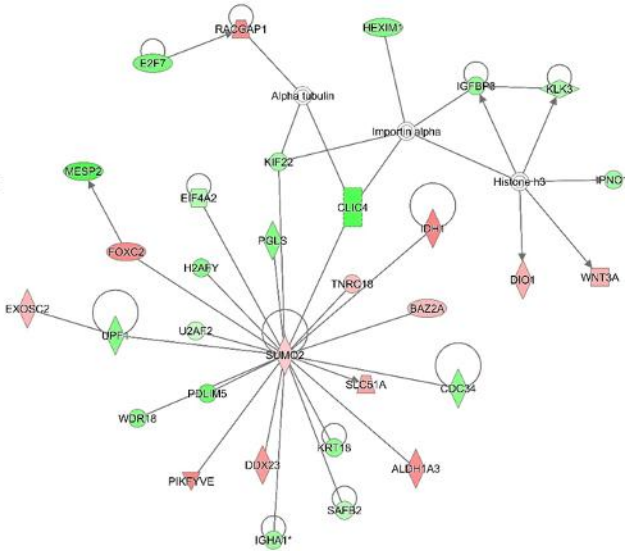

Gene Expression

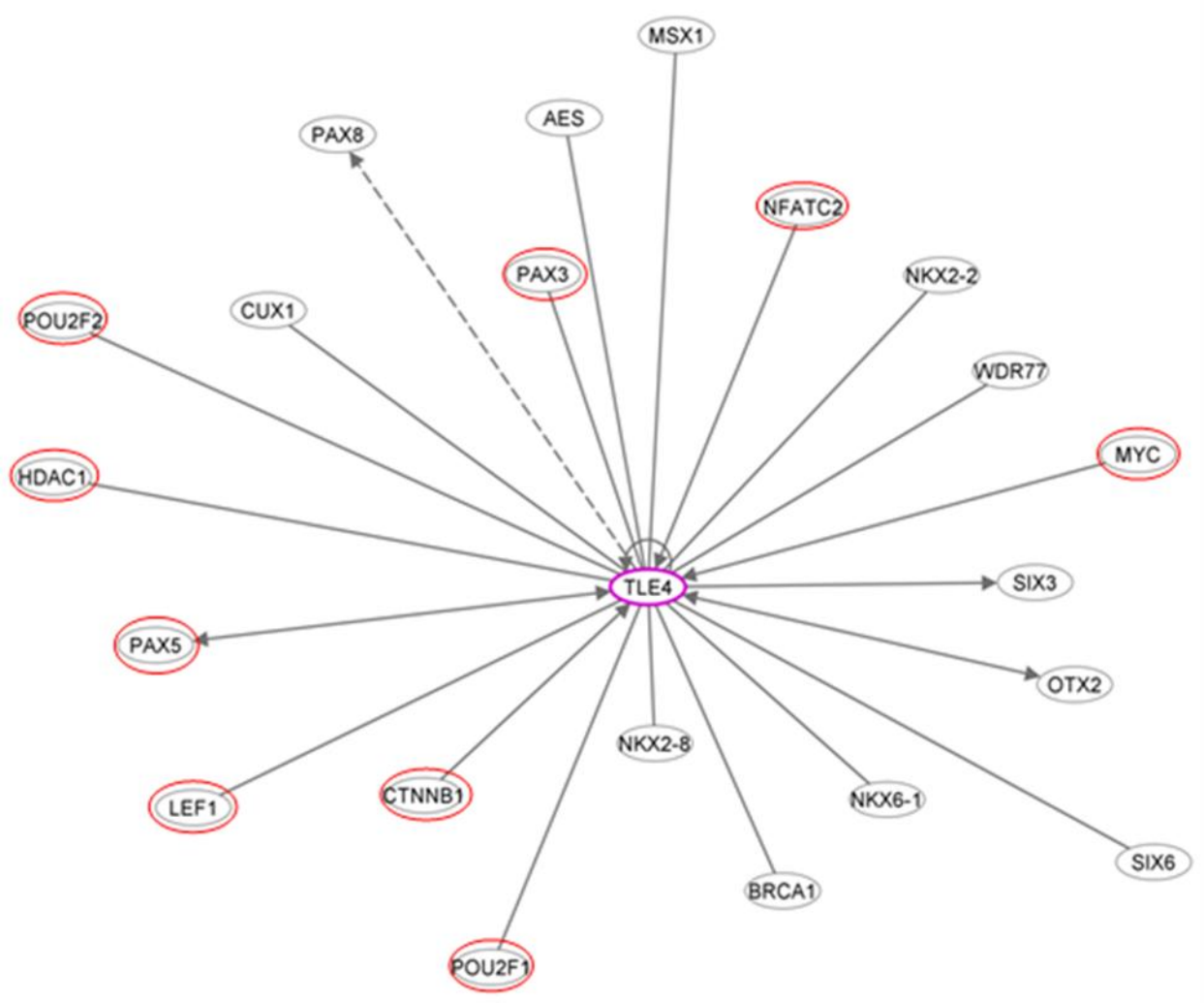
MSX1
AES
PAX8
NFATC2
PAX3
NKX2-2
CUX1
POU2F2
WDR77
MYC
HDAC1
TLE4
SIX3
PAX5
OTX2
NKX2-8
LEF1
CTNNB1
NKX6-1
SIX6
BRCA1
POU2F1